Journal of Sound and Vibration (1999) **219**(1), 51–62
Article No. jsvi.1998.1824, available online at http://www.idealibrary.com.on IDEAL

SEABOTTOM BACKSCATTER STUDIES IN THE WESTERN CONTINENTAL SHELF OF INDIA

B. Chakraborty and D. Pathak

National Institute of Oceanography, *Dona Paula*, *Goa* 403 004, *India*

(*Received* 23 *June* 1997, *and in final form* 12 *June* 1998)

In this paper, a study is initiated to observe the interaction effect of the sound signal with three different sediment bottoms in the shelf area between Cochin and Mangalore in the western continental shelf of India. An echo signal acquisition system has been designed and interfaced with the 12 kHz echosounder installed onboard ORV Sagar Kanya. The reflection coefficients including attenuation at the seawater/bottom interface are computed in the three different sediment areas based on the sediment mean grain size. The experimental coherent reflection coefficients are calculated using the attenuation corrected reflection coefficients and the normalized cross-correlation between successive backscatter echo signal waveforms in those areas. Further, analyses conducted by determining the echo peak Probability Density Function (PDF) and matching them with the experimental echo peak histograms provide root mean square (rms) roughness amplitude in the three different survey areas. The rms roughness values are used to compute the coherent reflection coefficients. An attempt to establish concurrence between the coherent reflection coefficients based upon the rms roughness amplitude and the experimental coherent reflection coefficients using the backscatter echo signals, reveals the importance of seawater/bottom interface roughness in the coarse grained sediment bottoms like sand and silty sand. The existence of microtopographic features are responsible for the seawater/bottom interface roughness. However, in the fine grained sediment area, the bottom does not contain any such feature.

1. INTRODUCTION

Sonar profiling of the seabed is a well known method for attaining objectives like characterization of the seabed and determining seafloor physical properties. The changes in bottom topography and roughness cause fluctuations in the backscattered signal. An analysis of the signal envelope fluctuation over several pings, i.e., transmission cycles, can be used to understand the roughness characteristics of the seafloor. In order to classify the seabed, the interaction effect of the bottom relief with the acoustical signal must be understood. Many workers [1–6] have contributed to identifying the bottom type from its reflection and scattering characteristics. Clay *et al*. [7] had used the echo envelope PDF (Probability Density Function) from a rough surface to estimate the coherent component of the backscattered signal. According to Stanton [5], using normal

0022–460X/99/010051 + 12 $30.00/0

incidence echo envelope statistics of the sounding device, microroughness (features like ripples, etc.; where the roughness amplitude is less than one-quarter of an acoustic wavelength) of the seafloor can be determined. This study is similar to the establishment of a relation between the specular to the diffused echo energy ratio (of the echo envelope) with the signal to noise ratio parameter of Rice distribution. Stanton demonstrated that the PDF of the echo amplitude is dependent on the seafloor roughness, sonar beam width and frequency.

In this paper, seabottom characteristics were determined using acoustic methods in conjunction with sediment sampling. An effort has been made to understand the interaction effect of the acoustic signal with three varying sediment type seabottoms in the shelf area between Cochin and Mangalore off the west coast of India. The experimental coherent reflections coefficient computed from the echo waveforms of the different seabottoms will vary according to the nature of the seabottom material and seabed roughness characteristics. An interface is developed for echo data acquisition to obtain the echo strength of the single beam echosounder (Honeywell-Elac) operating at 12 kHz installed onboard ORV Sagar Kanya. This interface is a modified form of the data acquisition system for the Sparker (shallow seismic system) signal. The overall sediment distribution is known in the areas where the present study is carried out [8]. The ground conditions in the area were rigorously studied earlier [9] and have been used for the present study.

Stanton's technique [5] of computing the PDF of the seabottom echopeak amplitude has been applied in this work Talukdar and Lawing [10] have developed a method to determine a factor (ratio of the coherently reflected energy to the incoherently scattered energy), which is a measure of the relative roughness or smoothness of the seabottom [5]. The computed factor is high for a smooth bottom while it is low for a rough bottom. For a rippled relief, the computed factor is a function of the root mean square (rms) roughness amplitude at the seawater/bottom interface, (i.e., the ripplie height) and hence can be used to determine the rms roughness amplitude in the different microtopographic provinces. Using rms roughness amplitudes, the coherent reflection coefficient of the different seabottoms are computed, and a comparison of these values with the experimental coherent reflection coefficient using echo waveform data, gives information about the rms roughness amplitudes of the seabed in the western continental margin of India. The results are in accordance with the geological information available from the ground conditions.

2. ECHO DATA ACQUISITION

The echo signal is acquired from the 12 kHz deepsea echosounder (Honeywell-Elac) by using an interface which is a modified version of the data acquisition system for the Sparker signal [11]. A block diagram of the echo signal acquisition system is shown in Figure 1. The echo signal is fed to the programmable delay circuit. The sounding trigger from the echosounder initializes the delay period. The dealy circuit tracks the received echo and a gate is set for the digitization of the complete pulse length. The pulse is sampled at a frequency

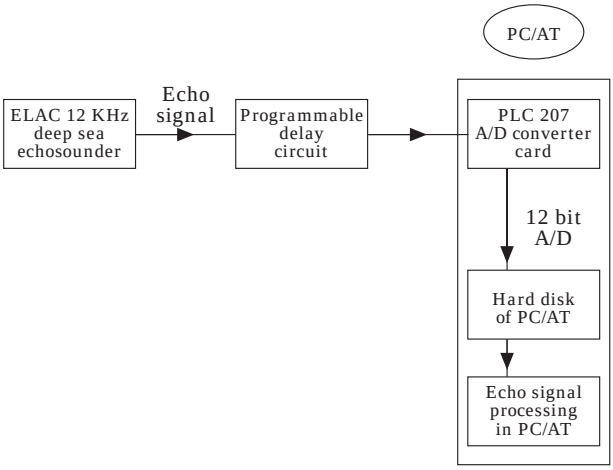

Figure 1. Block diagram of the Echo signal acquisition system.

of 50 kHz with the help of a PCL-718 high performance data acquisition card installed in the PC/AT. The A/D (analog to digital) conversion is performed in the external pulse trigger mode whereby the conversion begins on the arrival of the external pulse which is generated by the delay circuit electronics. The output of the PCL-718 is a 12 bit data signal which is stored in the PC hard disk. The instantaneous echo peak amplitude for each transmission is extracted. The rms value of the peak amplitude is used as a normalization factor and the normalized echo peak histograms are generated.

3. SURVEY AREA

Figure 2 represents the survey region between Cochin and Mangalore in the western continental shelf of India. Areas A and B consist of coarse grained sediments, i.e., sand and silty sand respectively. Area C is a fine grained clayey silt sediment. The sediment samples were collected during the RV Gaveshani cruises 30 and 207. The detailed sediment distribution is known in the three areas where the echo signal data is collected. Area A is located around 11°30′N and 75°06′E and the areas B and C are around 10°40′N, 75°25′E and 12°40′N, 74°40′E respectively. The total number of pings collected in the areas A, B and C are 400, 253 and 227 respectively. The water depths vary from 45 m to 60 m in the three areas. The selected transmission pulse length is 1 ms. The echo waveform data was collected during ORV Sagar Kanya cruise 74.

4. ANALYSIS

The Rice PDF of the echo peak amplitude E from the seabed is described as [5]

$$P(E) = [2E(1+\gamma)/\langle E^2\rangle] \exp\{-[(1+\gamma)E^2 + \gamma\langle E^2\rangle]/\langle E^2\rangle\} \mathrm{I}_0(q). \quad (1)$$

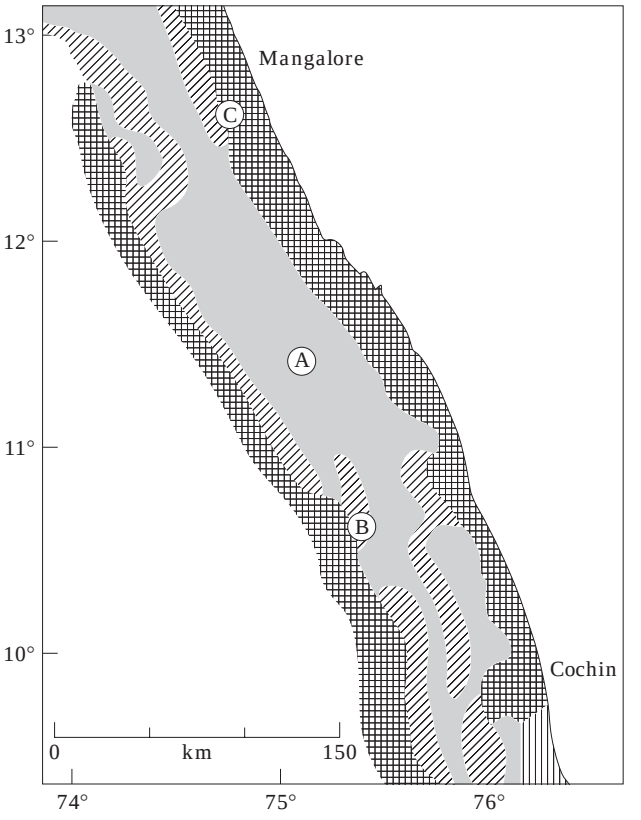

Figure 2. Sediment distribution map of the survey area. Key: ⊞, clayey silt; ▨, silty sand; ⊡, sand silt clay; ⬚, sand.

The term q in the modified Bessel function $I_0(q)$ can be expressed as

$$q = 2E[\gamma(1+\gamma)]^{0.5}/(\langle E^2\rangle)^{0.5}.$$

The expected value of the echo peak squared is denoted by $\langle E^2\rangle$, and γ is the measure of the relative roughness or smoothness of the seabottom. The Rice PDF is expressed with respect to γ and the appropriate selection of γ is used to fit the Rice PDF on the histograms of the echo peaks.

In order to determine the γ value of the different areas, a moment method based upon [10] is applied. One defines a new variable $y' = E/\sqrt{\langle E^2\rangle}$ and uses it in equation (1). The first moment (μ) of the Rice PDF [equation (1)] is expressed in terms of γ and y' as

$$\mu = \langle y'\rangle = \{\Gamma(3/2)/(1+\gamma)^{0.5}\}\exp(-\gamma/2)[(1+\gamma)I_0(\gamma/2) + \gamma I_1(\gamma/2)]. \qquad (2)$$

In the above equation, μ varies between $\sqrt{\pi/2}$ (Rayleigh PDF, $\gamma = 0$) and 1 (Gaussian PDF). The mean value of the peak data set is normalized with the second moment of the echo peak data, and is compared with the theoretical mean (μ, using equation 2) to obtain an estimated γ. Using the estimated γ value in equation (1), well matched PDF curves are plotted as seen in Figure 3. The histograms represent the experimental echo peaks while the curves describe the

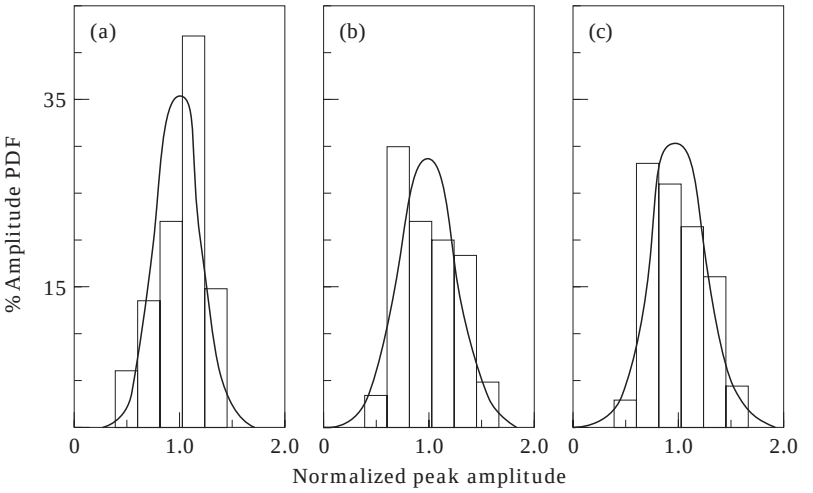

Figure 3. Probability density function of the echo peaks in the three different regions (a) sand, (b) silty sand and (c) clayey silt. Histograms represent the echo peaks while curves depict Rice PDFs for γ values (a) 11, (b) 6 and (c) 7 respectively.

theoretical PDFs. The PDFs are Gaussian in all the three areas and the narrowest PDF is obtained for the sandy bottom while the PDFs become broader for clayey silt and silty sand. γ, the measure of relative roughness or smoothness is found to be the highest for sandy bottom ($\gamma = 11$) and 7 and 6 for clayey silt (C) and silty sand (B) respectively. One observes that the scattering phenomena is minimum for the coarse grained sandy bottom area (A). Using simulated data, the accuracy of the moment method for curve matching is given in Talukdar and Lawing [10]. A similar study on the echo peak data in the three different sediment bottoms of our interest shows that γ and the second moment of the echo peak converge towards their respective mean values as the number of samples in their respective datasets increase. The standard deviation of γ and the second moment of the echo peak also reduces with an increase in the sample set. For sandy bottom, the standard deviation of γ is restricted under 1·10 and for silty sand and clayey silt, the standard deviation is contained within 1·30 and 0·60 respectively. It is certain that the shape of the PDF curve does not vary significantly for variation of γ in its range estimated above.

For a rippled seabottom, the term γ can be expressed as

$$\gamma^{-1} = (300/\pi)B^2K^4\eta\sigma^{4\cdot5}, \tag{3}$$

where B is the full power beamwidth in radians between the e^{-1} points of the transducer beampattern, K is the operating wavenumber and σ is the r.m.s. roughness amplitude of the seabottom. The term η is associated with the ripple type. B (full power beamwidth) is 0·43 radians (25·06 degrees) and K is computed for a frequency of 12 kHz. According to Clay and Leong [12], η varies between 1 and 5. The two values of η provide the limits for the ripple correlation length

ratios varying along two different axes in the horizontal plane [5]. The rms roughness amplitude (σ) in the three areas are calculated using equation (3), based on the assumption that the bottom consists of ripples. This assumption has been made in the absence of photographic evidence of the microroughness of the area but the likelihood of a large scale topographically flat area in the shelf consisting of coarse grained sediment being rippled is high [13]. The computed rms roughness of the three different areas are calculated and presented in Table 1. Using $\gamma = 11$ for the sandy bottom in equation (3), σ varies between 0·0066 m and 0·009 m (for $\eta = 5$ to $\eta = 1$ respectively). Similarly σ ranges from 0·0075 to 0·011 m for silty sand ($\gamma = 6$) and from 0·0073 to 0·010 m for clayey silt ($\gamma = 7$) respectively. These estimated values of σ are in accordance with the results reported for rippled seabottom [4, 5] and [14].

In order to compute the reflection coefficients including attenuation at the seawater/bottom interface, one needs geoacoustical parameters of the surficial sediments. Empirical relations have been used to estimate these geoacoustical parameters from the logarithmic mean grain size (M_z in ϕ units) measurements of the bulk sediments [15]. The ratio of the sediment mass density to water mass density (ρ) is given as

$$\rho = \begin{cases} -0{\cdot}0165406M_z^3 + 0{\cdot}2290201M_z^2 - 1{\cdot}1069031M_z + 3{\cdot}0455234, & 1 < M_z < 5{\cdot}3, \\ -0{\cdot}0012973M_z + 1{\cdot}1564755, & 5{\cdot}3 < M_z < 9{\cdot}0. \end{cases} \quad (4)$$

Similarly, v, the ratio of sediment sound speed to water sound speed is expressed as

$$v = \begin{cases} -0{\cdot}0014881M_z^3 + 0{\cdot}0213937M_z^2 - 0{\cdot}1382798M_z + 1{\cdot}3424740, & 1 < M_z < 5{\cdot}3, \\ -0{\cdot}0024324M_z + 1{\cdot}0018916, & 5{\cdot}3 < M_z < 9{\cdot}0. \end{cases} \quad (5)$$

The ratio values stated above are computed using the surficial mean grain size parameter (M_z) of the sediment bottom. The M_z values for sand, silty sand, and clayey silt sediment samples are determined as $1{\cdot}67\phi$, $2{\cdot}76\phi$, and $6{\cdot}57\phi$ respectively. M_z is expressed in ϕ units throughout this study. The attenuation coefficient, α (dB/m) is expressed as

$$\alpha = kf^n, \quad (6)$$

TABLE 1

The rms roughness, experimental, coherent and attenuation corrected reflection coefficients of the three different seabed provinces

Area	Rms roughness (m) for $\eta = 1$, $\eta = 5$ (σ)	Attenuation corrected reflection coefficient (R_0)	Experimental coherent reflection coefficient using echo waveforms	Coherent reflection coefficient for $\eta = 1$, $\eta = 5$ using rms roughness amplitude $\langle R \rangle$
Sand (A)	0·009, 0·0066	0·344	0·261	0·233, 0·278
Silty Sand (B)	0·011, 0·0075	0·204	0·131	0·112, 0·152
Clayey Silt (C)	0·010, 0·0073	0·062	0·035	0·037, 0·048

where f is the frequency in kHz, k and n are constants. Following [16], one assumes $n = 1$ in our study areas. The constant k is related to mean grain size (M_z) by the following relations:

$$k = \begin{cases} 0{\cdot}04556 + 0{\cdot}0245(M_z), & 0{\cdot}0 < M_z < 2{\cdot}6, \\ 0{\cdot}1978 + 0{\cdot}1245(M_z), & 2{\cdot}6 < M_z < 4{\cdot}5, \\ 8{\cdot}0399 - 2{\cdot}5228(M_z) + 0{\cdot}20098(M_z^2), & 4{\cdot}5 < M_z < 6{\cdot}0, \\ 0{\cdot}9431 - 0{\cdot}2041(M_z) + 0{\cdot}0117(M_z^2), & 6{\cdot}0 < M_z < 9{\cdot}5. \end{cases} \quad (7a\text{–}d)$$

Using equations (6) and (7a–d) the attenuation coefficients are computed. The sediment attenuation coefficients for sand, silty sand, and clayey silt are computed as 5·95, 6·51 and 1·29 dB/m respectively. The loss tangent, δ i.e., the ratio of imaginary wave number to the real wave number for the sediments is expressed as [15]

$$\delta = \{\alpha v c_1 \ln (10)\}/(f 40\pi). \quad (8)$$

c_1 the sound speed in water in the survey area is measured as 1536 m/s [17]. In order to be consistent with Mourad and Jackson [15], $c_1 = 1{\cdot}536$ m/ms has been used for the computation of δ. The attenuation corrected reflection coefficient $R_0(\theta)$ at the seawater/bottom interface is expressed as

$$R_0(\theta) = (y'' - 1)/(y'' + 1), \quad (9)$$

where θ is the grazing angle. y'' is defined as

$$y'' = (\rho \sin \theta)/p(\theta). \quad (10)$$

and $p(\theta)$ is written as

$$p(\theta) = [k'^2 - \cos^2 (\theta)]^{0{\cdot}5}. \quad (11)$$

Again, k' is given as

$$k' = (1/v)(1 + \mathrm{i}\delta). \quad (12)$$

$R_0(\theta)$ becomes a complex quantity due to the inclusion of the lossy term, δ in the model. $R_0(\theta)$ is computed as 0·344, 0·204 and 0·062 for sand, silty sand, and clayey silt respectively for a grazing angle of 90° using equations (4–12) (Table 1).

The echo waveform data obtained at three different sedimentary provinces using a 12 kHz echosounder was used to compute the experimental coherent reflection coefficient based on the method provided by Clay [2]. Clay computed the cross-correlation between e_1 (first echo signal in the dataset) and e_j ($j = 2, n$, successive echo signals) collected at a particular area and used the autocorrelation function of e_1 as the normalization factor. According to Dunsiger and McIsaac [18], the cross-correlation between two successive signals is normalized with the square root of the product of the autocorrelation function of the same two signals using zero delay. The normalized cross-correlation function, $\varphi_{j,j+1}$ for delay τ is given by

$$\varphi_{j,j+1}(\tau) = r_{j,j+1}(\tau)/[r'_j(0) \quad r'_{j+1}(0)]^{0{\cdot}5}. \quad (13)$$

where $r_{j,j+1}$, the cross-correlation between the jth and $(j+1)$th echo is defined by

$$r_{j,j+1}(\tau) = \langle e_j(t) e_{j+1}(t-\tau) \rangle. \tag{14}$$

The autocorrelation function, r_j' for zero delay is given by

$$r_j'(0) = \langle e_j^2(t) \rangle, \tag{15}$$

where $r_j'(0)$ is the energy in the echo waveform e_j.

In order to compute the normalized cross-correlation at the water/sediment interface, it becomes necessary to identify the first layer in a multilayered bottom. To demarcate the signal reflected from the first layer, the echo energy density has been plotted against the received pulse length as seen in Figure 4. It is observed that the silty sand and the clayey silt region contain more than one layer while in the sandy area, only one layer is present. In silty sand and clayey silt, the first layer at the water/sediment interface is approximately 1 ms in width as observed in Figure 4 (a plateau is noticed in the echo energy density curve at around 1 ms). Using 1 ms of the received pulse, an average of the maximum normalized cross-correlation coefficient between successive echoes is computed for sand, silty sand and clayey silt as 0·760, 0·643 and 0·567 respectively. Further, the average normalized cross-correlation coefficient is used for the computation of the experimental coherent reflection coefficient.

According to Tolstoy and Clay [19], the coherent reflection coefficient $\langle R \rangle$ is expressed as

$$\langle R \rangle = R_0 \exp(-2K^2\sigma^2). \tag{16}$$

Clay [2] had used an equivalence between the ratio $\langle R \rangle / R_0$ [equation (16)] and the normalized cross-correlation coefficient ($\varphi_{j,j+1}$) between echoes [equation (13)].

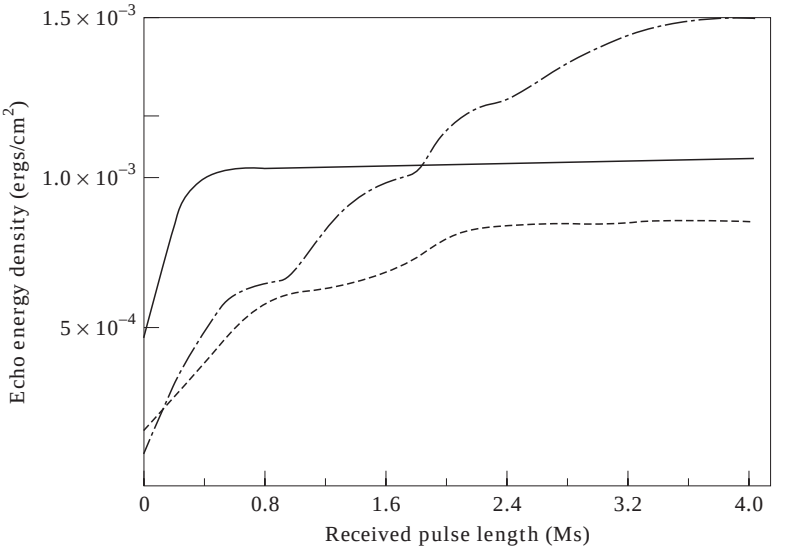

Figure 4. Echo energy density variation with the received echo pulse length. Key: —, sand; - - -, silty sand; – · – · –, clayey silt.

Using the earlier estimated values of $\varphi_{j,j+1}$ and R_0 [equation (9), $\theta = 90^\circ$ grazing angle] in this equivalence, the experimental coherent reflection coefficients using waveform data are computed as 0·261, 0·131 and 0·035 for sand, silty sand, and clayey silt respectively. We have extended our study to understand the influence of interface scattering at the seawater/bottom interface. Using two values of σ [(Table 1) for $\eta = 1$ and $\eta = 5$ equation (3)] in equation (16), two values of the coherent reflection coefficient $\langle R \rangle$ are obtained. These are 0·233 and 0·278 for sand, 0·112 and 0·152 for silty sand and 0·037 and 0·048 for clayey silt respectively. It is observed that the experimental coherent reflection coefficient lies within the bounds of the coherent reflection coefficient in the coarse grained sand and silty sand areas (see Table 1), which affirms that the seawater/bottom interface roughness is dominant in these areas and suggests the influence of microtopographic features. Conversely, in the fine grained clayey silt area, the experimental coherent reflection coefficient lies below the lower bound of the coherent reflection coefficient range. The authors have tried to reason the cause for this dissimilar behaviour in the fine grained clayey silt region. The bottom is of layered type here, as is evident from the echo energy density diagram (Figure 4). The presence of an acoustically transparent layer in a fine grained sediment area can contribute to the total echo significantly and to a higher normalized cross correlation. But, in the clayey silt area of the present interest, the normalized cross-correlation value is low, which may be due to a high proportion of internal scatterers i.e., volume inhomogeneity. The above studies suggest that the fine grained sediment in the present survey area does not signify any evidence of microtopographic features. Geologically too, in fine grained sediments, the cohesiveness is more and hence it is difficult to observe microtopographic features [20].

5. CONCLUSIONS

A study has been performed to understand the manner in which varying sediment type seabottoms of the shelf areas in the western continental shelf of India interact with a 12 kHz echosounder signal, and certain results have been inferred. Diverse methods like PDF determination, rms roughness evaluation and estimation of coherent reflection coefficients indicate that the seabottom in the three areas is relatively smooth. Using the Rice PDF study, the rms roughness height computed for a sandy bottom is found lower than those for silty and clayey silt. The rms roughness height values obtained for a relatively coarse grained sandy bottom area is comparable with the value provided in Briggs [21] for shallow water sites in the continental shelves around the United States. Furthermore, study is continued at the next stage of the paper to validate the computed rms roughness height values using PDF methods. The study is important especially for fine grained clayey silt seabottom area. Because of the dominant volume roughness in the fine sediment area, computed rms roughness height using PDF method may not reveal accurate rms roughness height value at the seawater/bottom interface. An investigation into the computed coherent reflection coefficients reveals that the interface scattering for the coarse grained sandy and silty sand areas are due to

microtopographic features. Because the experimental coherent reflection coefficient lies within the bounds of the coherent reflection coefficients (computed using rms roughness height of the Rice PDF study) for the sand and silty sand seabottom areas (Table 1), this study affirms the dominance of the scattering at the seawater/bottom interface for the sandy and silty sand bottom, whereas in the fine grained clayey silt area, the experimental coherent reflection coefficient lies below the lower bound of the coherent reflection coefficient range. The reason behind this dissimilar behavior in the fine grained clayey silt region is observed to be connected with the existing layered bottom in the fine grained clayey silt area and penetration of the sound signal. Using echo waveform data, the computed low normalized corss-correlation value from the clayey silt area confirms the presence of internal scatterers within the sediments i.e., the volume inhomogeneity (Jackson and Briggs, 1992). Geologically, the cohesiveness is dominant for fine grained sediment than the coarse grained, hence, the absence of microtopographic features in fine grained clayey silt area.

Using multibeam angular dependence backscatter data of varying sediment regions, the interface and volume scattering can be studied [22]. Applying composite roughness theory to the multibeam angular backscatter data may reveal roughness information about the surveyed seabottom and the geological processes, including physical properties of the seabottom [23]. Since multibeam echosounder provides high resolution and high density backscatter data, the authors plan to carry out such studies around the western continental shelf of India to provide detailed information about the geological processes.

ACKNOWLEDGMENTS

We express our gratitude to Dr. E. Desa, Director, and Dr. C. S. Murty, and R. R. Nair, Deputy Directors, NIO for their suggestions and encouragement in the completion of this work and also express sincere thanks to the scientists Dr. M. Veeraya, Dr. N. H. Hashimi, F. Almeida and G. S. Navelkar for the informative discussions they had with us. The help from D. Ilangovan, P. G. Mislankar, and V. D. Khedekar during sediment sample data analysis and echo data collection during RV Gavesheni cruises (30 and 207) and ORV Sagarkanya cruise (74) is also acknowledged. We are thankful to the anonymous reviewers for their useful suggestions to improve the work significantly. This is NIO's Contribution number 2573.

REFERENCES

1. C. M. McKinny and C. D. Anderson 1964 *Journal of the Acoustical Society of America* **36**, 158–163. Measurement of backscattering of sound from the ocean bottom.
2. C. S. Clay 1966 *Journal of Geophysical Research* **71**, 2037–2044. Coherent reflection of sound from the ocean bottom.
3. B. E. Bell and W. J. Porter 1974 *Physics of Sound in Marine Sediments*, New York: Plenum; see pp. 319–335.
4. A. D. Dunsiger, N. A. Cochrane and W. J. Vettor 1981 *IEEE Journal of Ocean Engineering* **6**, 94–107. Seabed characterization from broadband acoustic echosounding with scattering models.

5. T. K. Stanton 1984 *Journal of the Acoustical Society of America* **75**, 809–818. Sonar estimates of seafloor microroughness.
6. B. Chakraborty 1989 *Journal of the Acoustical Society of America* **85**, 1478–1481. Effects of scattering due to seafloor microrelief on a multifrequency-sonar seabed profiler.
7. C. S. Clay, H. Medwin and W. M. Wright 1973 *Journal of the Acoustical Society of America* **53**, 1677–1683. Specularly scattered sound in the probability density function of a rough surface.
8. R. R. Nair and N. H. Hashimi 1980 *Indian Academy of Sciences* (*Earth and Planetory Sciences*) *Proceedings* **89**, 299–315. Holocene climate inferences from the sediments of the Western India continental shelf.
9. R. R. Nair, N. H. Hashimi and V. P. Rao 1982 *Marine Geology* **50**, M1–M9. Distribution and dispersal of clay minerals on the western continental shelf of India.
10. K. K. Talukdar and W. D. Lawing 1991 *Journal of the Acoustical Society of America* **89**, 1193–1197. Estimation of the parameters of the Rice distribution.
11. D. Pathak 1991 *National Symposium on Ocean Electronics Proceeding*. Cochin: Cochin University of Science and Technology; see pp. 53–56.
12. C. S. Clay and W. K. Leong 1974 *Physics of Sound in Marine Sediments*. New York: Plenum; see pp. 373–446.
13. B. C. Heezen and C. D. Hollister 1971 *The Face of the Deep*. New York: Oxford.
14. T. K. Stanton and C. S. Clay 1986 *IEEE Journal of Ocean Engineering* **11**, 79–96. Sonar echo statistics as a remote sensing tool: volume and seafloor.
15. P. D. Mourad and D. R. Jackson 1989 *IEEE Oceans* '89 *Proceedings*. New York: IEEE; see pp. 1168–1175.
16. E. L. Hamilton 1972 *Geophysics* **37**, 620–646. Compressional wave attenuation in marine sediments.
17. S. P. Kumar, G. S. Navelkar, T. V. Ramanamurthy, Y. K. Somayajulu and C. S. Murty 1993 *Indian Journal of Marine Sciences* **22**, 17–20. Sound speed structure in the Arabian sea and Bay of Bengal.
18. A. D. Dunsiger and R. R. McIsaac 1978 *IEEE Oceans* '78 *Proceedings*. New York: IEEE; see pp. 521–526.
19. I. Tolstoy and C. S. Clay 1966 *Ocean Acoustics*: *Theory and Experiment in Underwater Sound*. New York: McGraw Hill.
20. R. R. Nair and N. H. Hashimi 1987 *Contributions in Marine Sciences—Dr. S. Z. Quasim Sixtieth Birthday Felicitation*. Goa: NIO; see pp. 413–425.
21. K. Briggs 1989 *IEEE Journal Ocean Engineering* **14**, 360–367. Microtopographical roughness of shallow water continental shelves.
22. C. D. Moustier and D. Alexandrou 1991 *Journal of the Acoustical Society of America* **90**, 522–531. Angular dependence of 12 kHz seafloor acoustic backscatter.
23. D. R. Jackson, D. P. Winebrenner and A. Ishimaru 1986 *Journal of the Acoustical Society of America* **79**, 1410–1422. Application of the composite roughness model to high frequency bottom backscattering.